Entanglement Activation in Multiphoton Distillation Networks

Yu-Ao Chen

yuaochen@ustc.edu.cn

University of Science and Technology of China https://orcid.org/0000-0002-2309-2281

Rui Zhang

University of Science and Technology of China https://orcid.org/0000-0001-5687-5576

Yue-Yang Fei

University of Science and Technology of China

Zhenhuan Liu

Tsinghua University

Xingjian Zhang

Tsinghua University

Xu-Fei Yin

University of Science and Technology of China

Yingqiu Mao

University of Science and Technology of China

Li Li

University of Science and Technology of China

Nai-Le Liu

University of Science and Technology of China

Xiongfeng Ma

Tsinghua University https://orcid.org/0000-0002-9441-4006

Jian-Wei Pan

University of Science and Technology of China https://orcid.org/0000-0002-6100-5142

Article

Keywords:

Posted Date: February 2nd, 2024

DOI: https://doi.org/10.21203/rs.3.rs-3828402/v1

Additional Declarations: There is **NO** Competing Interest.

Entanglement Activation in Multiphoton Distillation Networks

Rui Zhang[1,2,*], Yue-Yang Fei[1,2,*], Zhenhuan Liu[3,*], Xingjian Zhang[3], Xu-Fei Yin[1,2,4], Yingqiu Mao[1,2,4], Li Li[1,2,4], Nai-Le Liu[1,2,4], Xiongfeng Ma[3,4], Yu-Ao Chen[1,2,4] & Jian-Wei Pan[1,2,4]

[1]*Hefei National Research Center for Physical Sciences at the Microscale and School of Physical Sciences, University of Science and Technology of China, Hefei 230026, China.*

[2]*CAS Center for Excellence in Quantum Information and Quantum Physics, University of Science and Technology of China, Hefei 230026, China.*

[3]*Center for Quantum Information, Institute for Interdisciplinary Information Sciences, Tsinghua University, Beijing 100084, China.*

[4]*Hefei National Laboratory, University of Science and Technology of China, Hefei 230088, China.*

[*] *These authors contribute equally to this work.*

In quantum networks, residual states remaining after information processing can be valuable resources. Efficiently recycling these states to extract resources such as genuine multipartite entanglement and Einstein-Podolsky-Rosen pairs is essential for optimizing network performance. Our work demonstrates a tripartite entanglement distillation scheme using an eight-photon quantum platform, showcasing entanglement activation phenomena unique to multipartite systems. We successfully generate a three-photon genuinely entangled state from two bi-separable states through local operations and classical communication, illustrating multipartite entanglement activation. Furthermore, we extend our scheme to generate a three-photon state capable of extracting Einstein-Podolsky-Rosen pairs from two initial states lacking this capability, revealing a new entanglement activation phenomenon. Our findings offer not only practical applications for quantum networks but also a deeper theoretical understanding of multipartite entanglement structures.

Introduction. — In the future, quantum devices would form a global network, connecting remote clients through entanglement [1–3], likely facilitated by photon transmission [4]. Clients harness entanglement to carry out various information processing tasks, including quantum key distribution [5,6], quantum teleportation [7], and blind quantum computing [8]. Upon task completion, residual states would remain among different network nodes. Effectively recycling and converting these residual states into valuable quantum resources is key to enhancing network efficiency. Among these resources, Einstein-Podolsky-Rosen (EPR) pairs and genuine multipartite entanglement (GME), which respectively stand for the basic unit and global structure of entanglement, are the most crucial resources for multipartite quantum tasks [9–11].

Entanglement distillation [12,13], which transforms several less-entangled states into higher-entangled ones, is a primary technique for recycling resources. However, existing bipartite entanglement distillation schemes [14,15] may prove inadequate for handling general residual states in quantum networks, where quantum tasks generally involve multiple nodes. Moreover, compared with bipartite systems, certain distinguishing properties of multipartite entanglement could promise novel resource recycling approaches [16,17]. Entanglement activation, which shows that certain entanglement resources can be created by collecting multiple states without these resources, is a unique feature in multipartite systems [18,19]. Unlike in the bipartite systems, entanglement activation promises one to harvest something useful out of "nothing". To take advantage of activated entanglement resources, developing an effective multipartite distillation scheme is critical for resource recycling in quantum networks.

Multipartite entanglement distillation demands sophisticated multiphoton entanglement manipulation techniques. The spontaneous parametric down-conversion (SPDC) system stands out as the most mature quantum platform for preparing and manipulating multiphoton entangled states in multipartite quantum tasks [20]. However, the inherent probabilistic nature of the SPDC process gives rise to double-pair emission noises, which would introduce spurious contributions to experimental results. Such noise is a particularly notorious problem in entanglement distillation experiments and becomes more intricate as the photon number increases [14,15].

In this work, by delicately designing the entanglement distillation network into a crossed structure, we realize a tripartite entanglement distillation scheme which can filter out unwanted double-pair emission noises. Applying this scheme, we experimentally realize the entanglement recycling for multiphoton states and demonstrate two entanglement activation phenomena as sketched in Fig. 1. We first experimentally generate a three-photon genuinely tripartite entangled state from two copies of three-photon states without GME, demonstrating GME activation. In addition to GME, we define the *stochastic localizable entanglement* (SLE) to describe the ability to extract EPR pairs from given multipartite states through local operations and classical communication (LOCC) [21,22]. Through experimentally applying an additional single-photon measurement to the tripartite distillation scheme, we observe that SLE can also be generated by collecting two copies of states without SLE, showing a new entanglement activation phenomenon. To confirm our experimental findings, we theoretically derive the existence criterion for SLE and certify the SLE activation phenomenon.

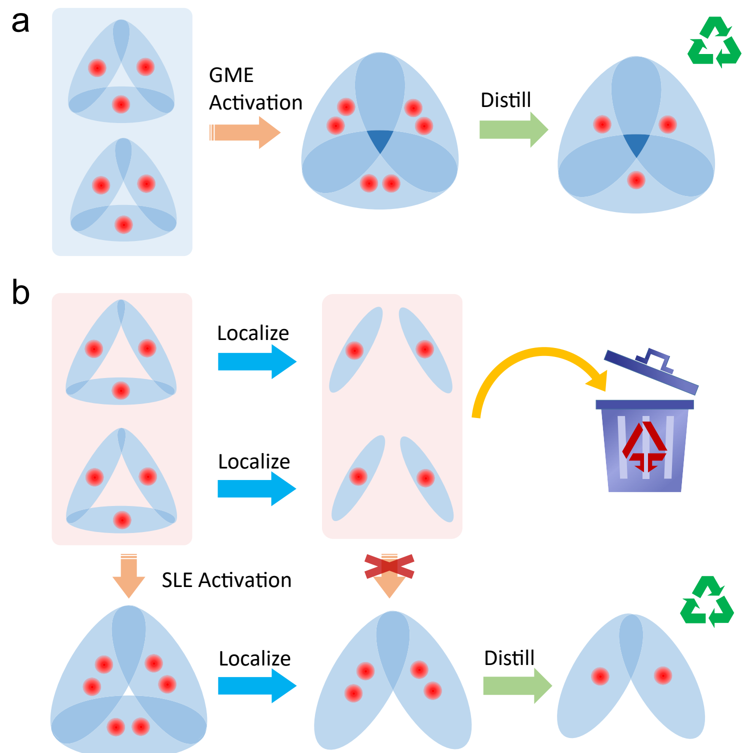

Figure 1: **Schematic of two types of entanglement activation in tripartite systems.** Red dots represent photons, and overlapping shaded areas indicate entanglement shared among subsystems. **a**, Genuine multipartite entanglement activation. GME can be activated by collecting two bi-separable tripartite states to form a new tripartite state. One can further perform tripartite distillation to recycle the resources. We use the common overlap of three shaded areas in deep blue to represent GME. **b**, Stochastic localizable entanglement activation. For some tripartite states, any LOCC localization protocol, such as measuring some subsystem, results in bipartite separable states shared between two subsystems. These resultant bipartite separable states, represented by two shaded areas without overlap, contain no resources for quantum networks. Similar to GME activation, when two copies of such tripartite states are collected, SLE can be activated and entanglement localization becomes possible.

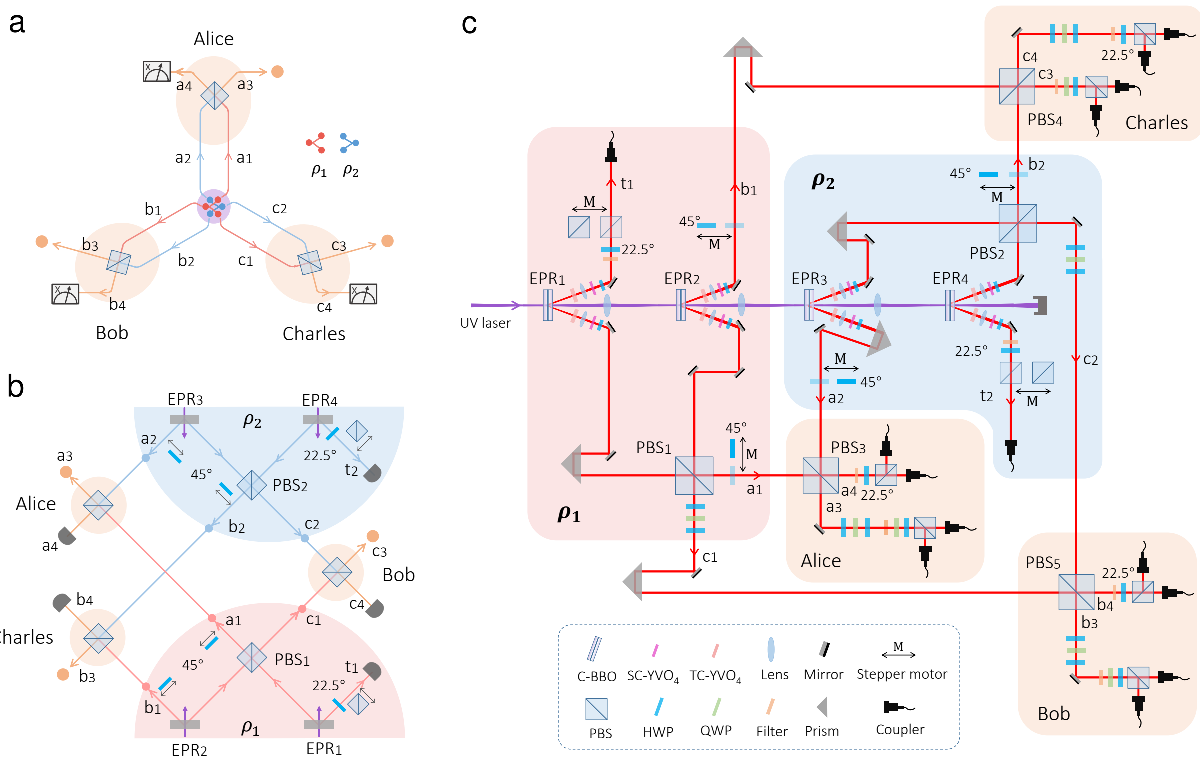

Figure 2: **Schematic of tripartite distillation scheme and experimental setup**. Blue and red areas represent the processes of preparing initial states, and orange areas represent distillation operations. **a**, Schematic of the tripartite entanglement distillation scheme. **b**, Schematic of the state preparation and distillation network for tripartite Werner states. **c**, Detailed experimental setup. Each to-be-distilled Werner state is independently prepared with two EPR sources. Three stepper motors are employed to drive a PBS and two HWPs to prepare different components of the Werner state. PBS_3, PBS_4, and PBS_5 are employed to realize the distillation operation by overlapping photons from two to-be-distilled states. The QWP-HWP-QWP combination after PBS is used to compensate for phase loss between two photons after interference on PBS. C-BBO: combination of β-barium borate crystals; SC-YVO_4: YVO_4 crystal for spatial compensation; TC-YVO_4: YVO_4 crystal for temporal compensation; HWP: half-wave plate; QWP: quarter-wave plate.

Experimental Scheme and Setup. — Based on previous advancements in entanglement distillation [12,13], we develop a tripartite distillation scheme, shown in Fig. 2. The initial states of the distillation scheme, ρ_1 and ρ_2, are prepared in three-qubit Werner states

$$\rho_{\text{werner}} = p\,|\text{GHZ}_3\rangle\langle\text{GHZ}_3| + (1-p)\frac{\mathbb{I}_3}{8}, \tag{1}$$

where $|\text{GHZ}_3\rangle = (|000\rangle + |111\rangle)/\sqrt{2}$ and $\frac{\mathbb{I}_3}{8}$ is the three-qubits maximally mixed state. Werner states can reflect the influence of unpredictable noise on quantum resources in networks and have a clear entanglement structure which would benefit the experimental demonstration of entanglement activation. By encoding $|0\rangle$ and $|1\rangle$ in the horizontal and vertical polarizations of photons, $|H\rangle$ and $|V\rangle$, the entanglement distillation can be achieved using the parity check function of polarizing beam splitter (PBS, transmitting $|H\rangle$ and reflecting $|V\rangle$) [13,14]. The overview of distillation procedures is shown in Fig. 2a. After the distribution of two initial states, labeled by a_1-b_1-c_1 and a_2-b_2-c_2, to Alice, Bob, and Charles, each of them introduces the two photons to a PBS and only keeps events where photons are emitted from both outputs of the PBS. Subsequently, each client performs the Pauli-X measurement on one of the two output photons, such as a_4-b_4-c_4, and compares measurement outcomes with others. If an even number of states $|-\rangle = (|H\rangle - |V\rangle)/\sqrt{2}$ is registered, they keep the remaining photons, a_3-b_3-c_3; otherwise, one of them applies the phase-flip operation to the remaining photon. After these procedures, the distilled state will acquire higher entanglement than the initial states.

Figure 2b sketches the Werner state preparation and entanglement distillation network within the linear optical platform. Each Werner state is prepared from two EPR pairs, generated via SPDC processes. Taking ρ_1 as an example, two photons from EPR_1 and EPR_2 are overlapped on PBS_1 to prepare a four-qubit GHZ state $|\text{GHZ}_4\rangle = (|H_{a_1}H_{b_1}H_{c_1}H_{t_1}\rangle + |V_{a_1}V_{b_1}V_{c_1}V_{t_1}\rangle)/\sqrt{2}$. Based on this state, three stepper motors are employed to prepare the three-qubit GHZ state and the maximally mixed state. One stepper motor randomly inserts a PBS into the light path of photon t_1 with a probability that depends on the parameter p of the target Werner state. When the PBS is in the light path, the heralding photon t_1 will be projected to $|+\rangle = (|H\rangle + |V\rangle)/\sqrt{2}$ and photons a_1-b_1-c_1 will be triggered to the $|\text{GHZ}_3\rangle$ state. When the PBS is out of the light path, the other two stepper motors will randomly insert two half-wave plates into the light paths of photons a_1 and b_1 to prepare the maximally mixed state $\frac{\mathbb{I}_3}{8}$. The movements of three stepper motors are not recorded, so that we can achieve the mixture of these two components in Eq. (1) and prepare the desired Werner state [23,24].

In practice, SPDC processes lead to the same-order double-pair emission events, where some

EPR sources yield two photon pairs while some yield no photons. Such events may also be registered and deviate the experiment from a faithful distillation procedure [14,15]. To filter out such events, the subsequent entanglement distillation network is delicately designed in a crossed structure. Therein, the heralding photons t_1 and t_2 ensure that both EPR_1 and EPR_4 sources generate exactly one photon pair; the arrangement of distillation PBSs makes sure that the double-pair emission of EPR_2 or EPR_3 cannot let all detectors respond, and the corresponding event is thus not recorded. This filtering strategy proves to be effective when preparing any component of the Werner state by introducing half-wave plates.

The detailed experimental setup is depicted in Fig. 2c. Four EPR sources are realized by successively targeting a beam of the pulsed ultraviolet laser through four sandwich-like combinations of β-barium borate crystals [25,26]. The pump laser is set with the central wavelength of 390 nm, repetition rate of 80 MHz, pulse duration of 150 fs, and pump power of 500 mW. For down-converted photons, to remove frequency distinguishability while maintaining a high counting rate, band-pass filters with the full width at half maximum of $\Delta\lambda = 4\ \mathrm{nm}$ are applied. As a result, the average counting rate of each EPR pair is 199,000 per second, and the average fidelity is 0.965. Photons from different EPR sources are finely adjusted to achieve temporal and spatial overlaps on distillation PBSs, leading to the Hong-Ou-Mandel-type interference. Consequently, fidelities of $|\mathrm{GHZ}_3\rangle$ states prepared on a_1-b_1-c_1 and a_2-b_2-c_2 reach 0.833 and 0.837, respectively; the interference visibilities of PBS_3, PBS_4, and PBS_5 used for distillation operation reach 79.6%, 78.8%, and 78.1%, respectively.

Results. — For Werner states, their GME can be determined using the entanglement witness [16]

$$W = \frac{1}{2}\mathbb{I}_3 - |\mathrm{GHZ}_3\rangle\langle\mathrm{GHZ}_3|\,, \tag{2}$$

which is equivalent to deciding whether the fidelity $F = \langle\mathrm{GHZ}_3|\,\rho\,|\mathrm{GHZ}_3\rangle$ exceeds 0.5. Besides, the preparation of GHZ states is crucial for many multiparty quantum information tasks. Thus, we adopt F as the target quantity to demonstrate the performance of our distillation scheme. Fig. 3a presents GME distillation results with Werner states of various values of p. Due to imperfections in state preparation, the prepared states deviate from the ideal Werner states, as depicted by blue and red lines in Fig. 3. Such imperfections also appear in real-world noisy quantum networks. Despite the deviation, the distillation operation exhibits significant improvements in fidelities, demonstrating the effectiveness of the distillation scheme. Taking states with $p = 0.6$ as an example, we generate a state with a fidelity of 0.612(31) from two less-entangled states with fidelities of 0.544 and 0.532.

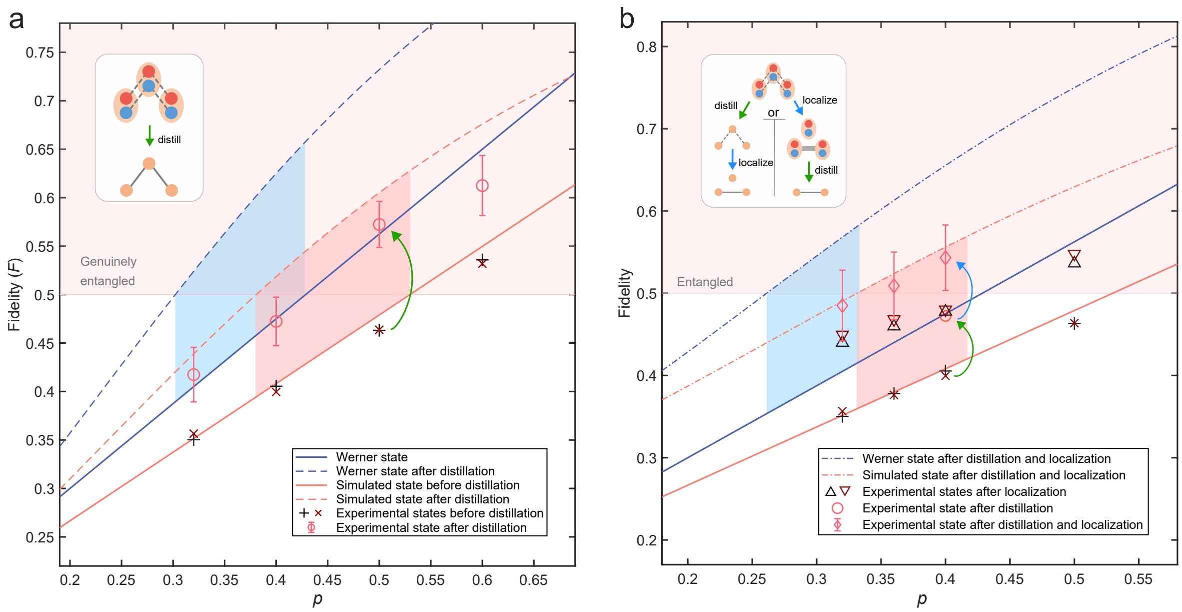

Figure 3: **Experimental results**. Blue solid lines are fidelities between ideal Werner states and $|\mathrm{GHZ}_3\rangle$ state. Red solid lines are fidelities of initial states simulated using the knowledge of noises in state preparation. Blue and red shadowed regions represent ranges of entanglement activation. **a**, Experimental results of the tripartite GME distillation. The blue and red dashed lines are calculated in the assumption of perfect distillation. Due to unpredictable noises in the state preparation and distillation, experimental results have certain deviations from simulated lines. The phenomenon of GME activation is demonstrated by states with $p = 0.5$, where the fidelity exceeds the GME threshold after distillation. **b**, Experimental results of the tripartite SLE distillation. The blue and red dash-dotted lines are calculated in the assumption of perfect distillation and localization with Pauli-X measurement. Triangles are fidelities of two-photon states extracted by individually localizing two initial states. Diamonds are fidelities of two-photon states extracted by tripartite distillation followed by localization. For two-photon states after the localization operation, their y-coordinate values represent fidelities with the EPR pair. States with $p = 0.5$ show that the localization operation can extract EPR pairs from noisy states without GME. States with $p = 0.4$ and $p = 0.36$ show the existence of states that can be used to extract EPR pairs only with the assistance of tripartite distillation. The right column of the inset provides another interpretation of our experiment procedure, a larger localization operation followed by the bipartite entanglement distillation. During the entire experiment, the operations of Charles are equivalent to a two-photon entangled measurement, which is independent of Alice and Bob. This entangled measurement localizes the whole state into a four-photon and bipartite entangled state. Based on the measurement result of Charles, Alice and Bob perform a bipartite entanglement distillation on their remaining state to extract the EPR pair.

For states with $p = 0.5$, the fidelities of the two initial states are 0.463 and 0.464, suggesting the possible absence of GME. After distillation, the fidelity is increased to $0.572(23)$, exceeding the GME threshold of 0.5 by more than three standard deviations. Since the distillation scheme employs solely LOCC protocols, which cannot generate GME from bi-separable states, this result provides experimental evidence for the activation of GME. To establish this conclusion rigorously, it is crucial to ensure the absence of GME in initial states, as noise in state preparation can significantly weaken the effectiveness of the entanglement witness [27]. For this purpose, we perform state tomography on two initial states. The tomographic data is shown in Supplementary Information. Based on the tomographic data and knowledge of the noise, we conduct two additional tests, namely, the GME concurrence [28,29] and the tripartite positive partial transposition criterion [30,31]. The results suggest the absence of GME in initial states, confirming the occurrence of GME activation. For the states with $p = 0.4$ and $p = 0.32$, although clear improvements in fidelities are also observed after distillation, their fidelities do not exceed 0.5. This shows that the activation of GME only exists in a narrow range.

In addition to GME, a multipartite state can possess other types of resources, like the ability to extract EPR pairs between different quantum network nodes. Such ability can be regarded as a basic property for an arbitrary multipartite mixed state defined as follows.

Definition (Stochastic Localizable Entanglement)**.** *A multipartite state ρ possesses stochastic SLE on subsystems A and B if and only if there exists a protocol with LOCC and post-selection on measurement results that transforms ρ into a bipartite entangled state shared between A and B.*

A direct corollary of this definition is that, similar to GME, SLE cannot be generated from any state without SLE through LOCC, as its definition already considers all possible LOCC protocols. Although lacking GME, some states in our experiment possess SLE, such as two initial states with $p = 0.5$, which means we can localize their entanglement into some subsystems and extract useful resources like EPR pairs. For an ideal three-photon Werner state, measuring one photon in Pauli-X basis is one of the optimal entanglement localization approaches. In our experiment, by projecting photons of Charles to $|+\rangle$ or $|-\rangle$ state, fidelities between the remaining two-photon states and EPR pair both exceed the bipartite entanglement threshold 0.5, as shown by two triangles of $p = 0.5$ in Fig. 3b.

Entanglement localization can be assisted by the tripartite distillation. As indicated by two triangles at $p = 0.4$, the localization operation fails to extract EPR pairs from both initial states with $p = 0.4$. Nevertheless, by adding the tripartite distillation operation on two initial states before the localization operation, the fidelity between the final two-photon state and the EPR pair exceeds 0.5. This process is indicated by the green arrow followed by the blue arrow. Therefore, we experimentally observe that the tripartite distillation enables the ability to extract EPR pairs.

Considering the deviation between experimentally prepared states and the ideal Werner state, measuring in Pauli-X basis may not be the optimal way to localize entanglement. Therefore, the failure of a specific localization operation cannot deny the existence of SLE, which should consider all possible localization protocols. To verify SLE of a given state, we derive a criterion in Methods section to reduce the search over all LOCC protocols to a much smaller set of localization operations, which only involves projective measurements. With this criterion, for initial states with $p = 0.36$, we confirm the absence of SLE using their tomographic data. After distillation and localization, we observe the fidelity between the remaining two-photon state and EPR pair exceeds 0.5. Considering that LOCC cannot create SLE, the experimental result indicates a new entanglement activation phenomenon.

Observation (SLE Activation)**.** *SLE can be activated by collecting multiple copies of a state without SLE.*

Inspired by this experimental observation, we adopt the ideal Werner state to theoretically prove the existence of SLE activation, shown in Supplementary Information.

Discussion and Outlook. — In this work, we have constructed a tripartite entanglement distillation network in an eight-photon linear optical platform, demonstrating two multipartite entanglement activation phenomena. SLE activation is first proposed and experimentally observed in this work, which provides a new direction for recycling resources. An essential consequence of SLE activation is that the amount of resources extracted from a given multipartite state may depend on the order of operations. For example, for states with SLE activation, performing entanglement localization before distillation may even destroy all entanglement resources.

Concepts of SLE and SLE activation also provide new viewpoints for understanding entanglement structure in multipartite systems. SLE extends concepts of entanglement of assistance [32] and localizable entanglement [22,33] and provides the object for these two quantifiers. Although SLE seems to represent a lower level of multipartite entanglement, Ref. [34] found a genuine multipartite entangled state, which has no SLE according to our criterion and shows the independence of SLE and GME. In the context of higher-dimensional multipartite states, SLE is not equivalent to the ability to extract EPR pairs due to the existence of bound entanglement [35]. Thus, it is worth further modifying the definition of SLE to adjust various tasks. It has been proved that, for multipartite states with specific properties, GME can always be activated by collecting sufficient copies [36]. Finding the conditions for SLE activation is still an intriguing open problem.

Acknowledgement

We appreciate insightful discussions with Otfried Gühne, Jens Eisert, Satoya Imai, Hayata Yamasaki, Xiaodong Yu, Luo-Kan Chen, and Feihu Xu. This work was supported by the National Natural Science Foundation of China (Grants No. 11975222, No. 11874340, No. 12174216), Shanghai Municipal Science and Technology Major Project (Grant No. 2019SHZDZX01), Chinese Academy of Sciences and the Shanghai Science and Technology Development Funds (Grant No. 18JC1414700), and the Innovation Program for Quantum Science and Technology (Grant No. 2021ZD0301901, No. 2021ZD0300804). Xu-Fei Yin was support from the China Postdoctoral Science Foundation (Grant No. 2023M733418). Yu-Ao Chen was supported by the XPLORER PRIZE from Tencent Foundation.

Competing financial interests

The authors declare no competing financial interests.

Methods

Genuine multipartite entanglement. — Genuine multipartite entanglement represents the global entanglement among all subsystems and is the highest level of multipartite entanglement [17]. Specifically, an N-partite state ρ is said to be genuinely multipartite entangled iff it cannot be decomposed as

$$\rho = \sum_{g\subset[N]} \sum_{i} p_g^i \rho_g^i \otimes \rho_{\bar{g}}^i, \tag{3}$$

where g denotes a nontrivial subset of the N parties, $\bar{g} = [N] - g$ is the complementary of g, $\{p_g^i\}_{g,i}$ is a probability distribution satisfying $\sum_{g,i} p_g^i = 1$ and $p_g^i \geq 0$, ρ_g^i and $\rho_{\bar{g}}^i$ are quantum states defined on systems g and $\bar{g}$. When $N = 2$, this definition reduces to the definition of bipartite entanglement.

Certification of SLE. — By definition, certificating SLE of a given state needs to ensure an LOCC operation with post-selection, i.e., a stochastic LOCC (SLOCC) operation, which can extract local bipartite entanglement from the state. An N-partite SLOCC operation can be written as

$$\Lambda(\rho) = \sum_i \left(K_1^i \otimes \cdots \otimes K_N^i\right) \rho \left(K_1^i \otimes \cdots \otimes K_N^i\right)^\dagger, \tag{4}$$

where $K^i = K_1^i \otimes \cdots \otimes K_N^i$ is the Kraus operator satisfying $\sum_i K^{i\dagger} K^i \leq \mathbb{I}$. As searching over all SLOCC operations is extremely challenging, we use the following theorem to reduce it into an easier search problem.

Theorem (SLE Verification Criterion)**.** *An N-partite state ρ possesses SLE on subsystems A and B if and only if there exists a pure tensor state $|\psi\rangle = \bigotimes_{g\in\overline{AB}} |\psi_g\rangle$ defined on the complementary set $\overline{AB}$, such that $\rho_{AB} = \frac{\langle\psi|\rho|\psi\rangle}{\mathrm{tr}(\langle\psi|\rho|\psi\rangle)}$ is an entangled state.*

Proof. If ρ_{AB} defined above is entangled, one can perform POVM measurements $\{|\psi_g\rangle\langle\psi_g|, \mathbb{I} - |\psi_g\rangle\langle\psi_g|\}_g$ on all the other subsystems. After measurement, ρ_{AB} is kept only when other subsystems get results of $\{|\psi_g\rangle\langle\psi_g|\}_g$. Through this SLOCC protocol, one successfully produces $\rho_{AB} = \frac{\langle\psi|\rho|\psi\rangle}{\mathrm{tr}(\langle\psi|\rho|\psi\rangle)}$, where $|\psi\rangle = \bigotimes_{g\in\overline{AB}} |\psi_g\rangle$, from ρ and the entanglement of ρ_{AB} shows that ρ indeed has SLE.

By definition, if ρ has SLE on subsystems A and B, there exists an SLOCC operation with separable Kraus operators $\{K^i = K_A^i \otimes K_B^i \otimes \cdots\}_i$ such that

$$\frac{\mathrm{tr}_{\overline{AB}}(\sum_i K^i \rho K^{i\dagger})}{\mathrm{tr}\left(\sum_j K^j \rho K^{j\dagger}\right)} = \sum_i \frac{\mathrm{tr}_{\overline{AB}}(K^i \rho K^{i\dagger})}{\mathrm{tr}\left(\sum_j K^j \rho K^{j\dagger}\right)} \tag{5}$$

is an entangled state on A and B. As the set of separable states is convex, there exists at least one Kraus operator $K = \bigotimes_{g\in[N]} K_g$, such that

$$\frac{\mathrm{tr}_{\overline{AB}}\left(K\rho K^\dagger\right)}{\mathrm{tr}\left(K\rho K^\dagger\right)} = \frac{(K_A \otimes K_B)\,\mathrm{tr}_{\overline{AB}}\left[\left(\bigotimes_{g\in\overline{AB}} K_g\right)\rho\left(\bigotimes_{g\in\overline{AB}} K_g^\dagger\right)\right](K_A \otimes K_B)^\dagger}{\mathrm{tr}\left(K\rho K^\dagger\right)} \tag{6}$$

is an entangled state. As SLOCC cannot activate bipartite entanglement, this means that $\mathrm{tr}_{\overline{AB}}\left[\left(\bigotimes_{g\in\overline{AB}} K_g\right)\rho\left(\bigotimes_{g\in\overline{AB}} K_g^\dagger\right)\right]$ is an unnormalized entangled state. According to the singular value decomposition, we can decompose K_g as $K_g = \sum_i \sqrt{\lambda_g^{i_g}} \left|v_g^{i_g}\right\rangle\left\langle u_g^{i_g}\right|$ where $\sqrt{\lambda_g^{i_g}} \geq 0$ is the singular value of K_g, $\{\left|u_{i_g}\right\rangle\}_i$ and $\{\left|v_{i_g}\right\rangle\}_i$ are sets of mutually orthogonal states. Substituting the singular value decomposition, we have

$$
\begin{aligned}
&\operatorname{tr}_{\overline{AB}}\left[\left(\bigotimes_{g\in\overline{AB}} K_g\right)\rho\left(\bigotimes_{g\in\overline{AB}} K_g^{\dagger}\right)\right] \\
&=\left(\sum_{g\in\overline{AB}}\sum_{i_g,j_g}\right)\left(\prod_{g\in\overline{AB}}\sqrt{\lambda_g^{i_g}\lambda_g^{j_g}}\left\langle v_g^{j_g}\middle|v_g^{i_g}\right\rangle\right)\left(\bigotimes_{g\in\overline{AB}}\left\langle u_g^{i_g}\right|\right)\rho\left(\bigotimes_{g\in\overline{AB}}\left|u_g^{j_g}\right\rangle\right) \qquad (7)\\
&=\left(\sum_{g\in\overline{AB}}\sum_{i_g}\right)\left(\prod_{g\in\overline{AB}}\lambda_g^{i_g}\right)\left(\bigotimes_{g\in\overline{AB}}\left\langle u_g^{i_g}\right|\right)\rho\left(\bigotimes_{g\in\overline{AB}}\left|u_g^{i_g}\right\rangle\right),
\end{aligned}
$$

where we use the property of $\left\langle v_g^{j_g}\middle|v_g^{i_g}\right\rangle=\delta_{i,j}$. As $\prod_{g\in\overline{AB}}\lambda_g^{i_g}\geq 0$, if the state in Eq. (7) is entangled, at least one element in the summation, $\left(\bigotimes_{g\in\overline{AB}}\left\langle u_g^{i_g}\right|\right)\rho\left(\bigotimes_{g\in\overline{AB}}\left|u_g^{i_g}\right\rangle\right)$, is entangled. This concludes our proof.

□

Reference

1. Simon, C. Towards a global quantum network. *Nature Photonics* **11**, 678–680 (2017).

2. Storz, S. *et al.* Loophole-free bell inequality violation with superconducting circuits. *Nature* **617**, 265–270 (2023).

3. Sahu, R. *et al.* Entangling microwaves with light. *Science* **380**, 718–721 (2023).

4. Pan, J.-W. *et al.* Multiphoton entanglement and interferometry. *Rev. Mod. Phys.* **84**, 777–838 (2012).

5. Bennett, C. H. & Brassard, G. Quantum cryptography: Public key distribution and coin tossing. In *Proceedings of IEEE International Conference on Computers, Systems and Signal Processing*, 175–179 (Bangalore, India, 1984).

6. Ekert, A. K. Quantum cryptography based on bell's theorem. *Phys. Rev. Lett.* **67**, 661–663 (1991).

7. Bennett, C. H. *et al.* Teleporting an unknown quantum state via dual classical and einstein-podolsky-rosen channels. *Phys. Rev. Lett.* **70**, 1895–1899 (1993).

8. Barz, S. *et al.* Demonstration of blind quantum computing. *Science* **335**, 303–308 (2012).

9. Horodecki, R., Horodecki, P., Horodecki, M. & Horodecki, K. Quantum entanglement. *Rev. Mod. Phys.* **81**, 865–942 (2009).

10. Zhong, Y. *et al.* Deterministic multi-qubit entanglement in a quantum network. *Nature* **590**, 571–575 (2021).

11. Pompili, M. *et al.* Realization of a multinode quantum network of remote solid-state qubits. *Science* **372**, 259–264 (2021).

12. Bennett, C. H. *et al.* Purification of noisy entanglement and faithful teleportation via noisy channels. *Phys. Rev. Lett.* **76**, 722–725 (1996).

13. Pan, J.-W., Simon, C., Brukner, Č. & Zeilinger, A. Entanglement purification for quantum communication. *Nature* **410**, 1067–1070 (2001).

14. Pan, J.-W., Gasparoni, S., Ursin, R., Weihs, G. & Zeilinger, A. Experimental entanglement purification of arbitrary unknown states. *Nature* **423**, 417–422 (2003).

15. Chen, L.-K. *et al.* Experimental nested purification for a linear optical quantum repeater. *Nature Photonics* **11**, 695–699 (2017).

16. Gühne, O. & Tóth, G. Entanglement detection. *Physics Reports* **474**, 1–75 (2009).

17. Lu, H. *et al.* Entanglement structure: Entanglement partitioning in multipartite systems and its experimental detection using optimizable witnesses. *Phys. Rev. X* **8**, 021072 (2018).

18. Huber, M. & Plesch, M. Purification of genuine multipartite entanglement. *Phys. Rev. A* **83**, 062321 (2011).

19. Yamasaki, H. *et al.* Activation of genuine multipartite entanglement: Beyond the single-copy paradigm of entanglement characterisation. *Quantum* **6**, 695 (2022).

20. Pan, J.-W. *et al.* Multiphoton entanglement and interferometry. *Rev. Mod. Phys.* **84**, 777–838 (2012).

21. Chitambar, E., Leung, D., Mančinska, L., Ozols, M. & Winter, A. Everything you always wanted to know about locc (but were afraid to ask). *Communications in Mathematical Physics* **328**, 303–326 (2014).

22. Popp, M., Verstraete, F., Martín-Delgado, M. A. & Cirac, J. I. Localizable entanglement. *Phys. Rev. A* **71**, 042306 (2005).

23. Amselem, E. & Bourennane, M. Experimental four-qubit bound entanglement. *Nature Physics* **5**, 748–752 (2009).

24. Dakić, B. *et al.* Quantum discord as resource for remote state preparation. *Nature Physics* **8**, 666–670 (2012).

25. Wang, X.-L. *et al.* Experimental Ten-Photon Entanglement. *Physical Review Letters* **117**, 210502 (2016).

26. Li, Z.-D. *et al.* Experimental quantum repeater without quantum memory. *Nature Photonics* **13**, 644–648 (2019).

27. Liu, P., Liu, Z., Chen, S. & Ma, X. Fundamental limitation on the detectability of entanglement. *Phys. Rev. Lett.* **129**, 230503 (2022).

28. Ma, Z.-H. *et al.* Measure of genuine multipartite entanglement with computable lower bounds. *Phys. Rev. A* **83**, 062325 (2011).

29. Hashemi Rafsanjani, S. M., Huber, M., Broadbent, C. J. & Eberly, J. H. Genuinely multipartite concurrence of n-qubit x matrices. *Phys. Rev. A* **86**, 062303 (2012).

30. Peres, A. Separability criterion for density matrices. *Phys. Rev. Lett.* **77**, 1413–1415 (1996).

31. Jungnitsch, B., Moroder, T. & Gühne, O. Taming multiparticle entanglement. *Phys. Rev. Lett.* **106**, 190502 (2011).

32. DiVincenzo, D. P. *et al.* Entanglement of assistance. In *Quantum Computing and Quantum Communications*, 247–257 (Springer Berlin Heidelberg, Berlin, Heidelberg, 1999).

33. Verstraete, F., Popp, M. & Cirac, J. I. Entanglement versus correlations in spin systems. *Phys. Rev. Lett.* **92**, 027901 (2004).

34. Miklin, N., Moroder, T. & Gühne, O. Multiparticle entanglement as an emergent phenomenon. *Phys. Rev. A* **93**, 020104 (2016).

35. Horodecki, M., Horodecki, P. & Horodecki, R. Mixed-state entanglement and distillation: Is there a "bound" entanglement in nature? *Phys. Rev. Lett.* **80**, 5239–5242 (1998).

36. Palazuelos, C. & Vicente, J. I. d. Genuine multipartite entanglement of quantum states in the multiple-copy scenario. *Quantum* **6**, 735 (2022).

Supplementary Files

This is a list of supplementary files associated with this preprint. Click to download.

- SIEntanglementActivation.pdf